

## Influence of the Hydrogen Reduction Time and Temperature on the Morphology Evolution and Hematite/Magnetite Conversion of Spindle-Type Hematite Nanoparticles

Thierry Chappuis<sup>\*a</sup>, Izabela Bobowska<sup>a</sup>, Stefan Hengsberger<sup>a</sup>, Ennio Vanoli<sup>a</sup>, and Hervé Dietsch<sup>\*b</sup>

<sup>\*</sup>Correspondence: Prof. Dr. T. Chappuis<sup>a</sup>, Dr. H. Dietsch<sup>b</sup>

<sup>a</sup>Ecole d'Ingénieurs et d'Architectes de Fribourg, Boulevard de Pérolles 80, CP 32 CH-1705 Fribourg

Tel.: +41 26 429 67 14, E-mail: thierry.chappuis@hefr.ch

<sup>b</sup>University of Fribourg, Adolphe Merkle Institute, Route de l'Ancienne Papeterie, P.O. BOX 209, CH-1723 Marly 1

Tel.: +41 26 300 91 37, E-mail: herve.dietsch@unifr.ch

**Abstract:** We report on the transformation *via* hydrogen reduction of spindle-type hematite nanoparticles into hematite/magnetite hybrid iron oxide particles. The transformation process consists of the reduction of nanoparticles powder in an autoclave using hydrogen gas at a fixed pressure of 11 bars. Both temperature and time of reduction are varied between 300 °C to 360 °C and 0 to 45 h. X-Ray powder diffraction data on the obtained powder and corresponding Rietveld refinement allow the amount of reduced hematite to be determined as a function of these two parameters. Kinetics parameters are measured and an estimation of the activation energy is obtained through linearization of the Arrhenius equation. While reduction is dramatically accelerated at higher temperature, the morphology of the nanoparticles only remain qualitatively unchanged at 300 °C as seen from transmission electron microscopy images. The mechanisms underlying morphology changes are still under study and seem to be closely related to reactor pressure.

**Keywords:** Anisotropic nanoparticles · Hematite · Hybrid structure · Hydrogen reduction · Iron oxide nanoparticles · Magnetite

### 1. Introduction

Among iron oxide magnetic nanoparticles,  $\alpha$ -Fe<sub>2</sub>O<sub>3</sub> (hematite) and Fe<sub>3</sub>O<sub>4</sub> (magnetite) represent the most studied crystalline phases<sup>[1–4]</sup> for their use in both fundamental studies<sup>[5]</sup> such as control of colloidal stability and interactions<sup>[6]</sup> or better understanding of magnetic properties<sup>[7]</sup> and numerous applications in the field of catalysis,<sup>[8]</sup> information storage,<sup>[9]</sup> drug delivery,<sup>[10]</sup> purification techniques for the separation of cells or proteins,<sup>[11]</sup> or in the design of hybrid organic-inorganic materials that react to different types of stimuli.<sup>[12–15]</sup>

At room temperature, nanoparticles of hematite only exhibit weak magnetic properties. They are canted anti-ferromagnetic.<sup>[7]</sup> Although their interest is *a priori* limited by exhibiting low magnetic response, many methods exist in order to synthesize them with various sizes and shapes<sup>[4,16–18]</sup> and the formation of anisotropic hematite nanoparticles with relatively large aspect ratios is easily achieved by wet chemistry methods.<sup>[1]</sup> The ability to form hematite nanoparticles with anisotropic shapes can be a decisive advantage in some applications. In particular, magnetic nanoparticles with a high aspect ratio, like the ellipsoidal hematite

nanoparticles presented in this study, are of particular interest because of their ability to be oriented by an external magnetic field.<sup>[19]</sup> Thus, such particles have the ability to be able to orient and polarize light or X-rays.<sup>[20]</sup>

Unlike hematite nanoparticles, magnetite nanoparticles show a very strong magnetic response due to their strongly ferrimagnetic and even superparamagnetic (in the case of crystals smaller than 15 nm) properties.<sup>[5]</sup> However, limitations lie in the synthesis of these particles in a wide range of sizes and morphologies. Therefore, despite their interesting magnetic behavior, widespread use of magnetite nanoparticles appears limited by size and shape customization.

We recently proposed a method for the transformation of spindle-type hematite nanoparticles into hematite/magnetite hybrid iron oxide nanoparticles with tunable magnetic responses.<sup>[21]</sup> This proof of concept was done by fixing experimental parameters such as temperature and pressure of the reactor and the single varied parameter was the time of reduction in the autoclave process. As a result, magnetic properties were found to be tunable, morphology was qualitatively maintained and 45 h were found to be necessary to reach a 96 wt% of the hematite into magnetite. In this context, the present study focuses on the optimization of the necessary transformation time by studying the temperature influence on the kinetics of reaction and in parallel reporting on the final morphology changes influenced by temperatures of transformation.

### 2. Experimental Section

#### 2.1 Synthesis of Spindle-shaped Hematite Nanoparticles

Spindle-shaped hematite ( $\alpha$ -Fe<sub>2</sub>O<sub>3</sub>) nanoparticles are synthesized by forced hydrolysis of Fe(ClO<sub>4</sub>)<sub>3</sub> according to a procedure previously described by Ocaña *et al.*<sup>[1]</sup> In a typical synthesis, a 15-L working volume Hastelloy reactor equipped with a mechanical stirrer and a double jacket heating system is used. 693.6 g of Fe(ClO<sub>4</sub>)<sub>3</sub>·6H<sub>2</sub>O (reagent grade, Alfa Aesar, 1.5 mol), 90.07 g of urea (p.a., Sigma-Aldrich, 1.5 mol) and 9.73 g of Na<sub>2</sub>HPO<sub>4</sub> (>98% Sigma-Aldrich, 0.081 mol) are dissolved in 15 L ultrapure water (Arium, resistivity = 18.2 MΩ·cm) and heated at 100 °C for 24 h. A precipitate is collected by centrifuging at 10 000 rpm for 8 min. The precipitate is further washed 5 times with Ultrapure water repeating the centrifugation step, while supernatant is discarded each time. The remaining powder is then dried in an oven at 100 °C for two days at atmospheric pressure. The collected mass of hematite particles is typically of 13.5 g (11.3% yield based on the initial amount of iron perchlorate).

#### 2.2 Reducing Hematite Spindle-shaped Nanoparticles into Hematite/Magnetite

The reduction of the hematite spindle-shaped nanoparticles is performed in a custom-made (elements provided by Swagelog) 10 mL autoclave installation that is connected alternatively to a hydrogen cylinder or a nitrogen cylinder for flushing (Fig. 1). Each reduction experiment is carried out as follows: 0.2 g of hematite spindles powder is placed in the autoclave. The autoclave is flushed five times with nitrogen gas at 8.5 bars, subsequently

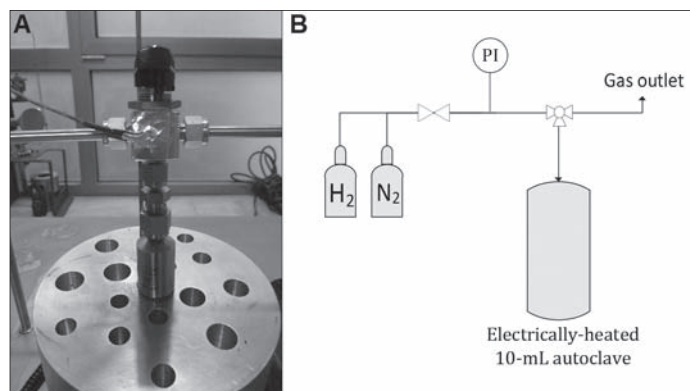


Fig. 1. (A) Digital image and (B) schematic representation of the experimental setup used to reduce in an autoclave using hydrogen gas spindle-shaped hematite nanoparticles into hybrid hematite/magnetite ones.

replaced by flushing five times with hydrogen gas. The hematite particles powder is then heated at a temperature of 300 °C, 340 °C or 360 °C in the hydrogen atmosphere under a constant pressure of 11 bars. Temperature and pressure are maintained for periods of time varying between 1 and 45 h.

### 2.3 Analytical Methods

Imaging and morphology changes of both hematite and hematite/magnetite hybrid nanoparticles are characterized using a transmission electron microscope (TEM-CM100, Philips) operating at 80 kV.

Powder X-ray diffraction patterns of the samples are measured with a Philips, PW1800 diffractometer (Cu-tube, 40kV, 40mA, step scan mode 0.02°/step, 2sec/step, 2Theta = 15–140°). The obtained XRD spectra are fitted employing the two most probable crystalline structures (hematite and magnetite) as references and using the Rietveld method as described in our previous work.<sup>[21]</sup> Rietveld refinement is done with the TOPAS3 software package (Bruker Inc.) using the fundamental parameter approach. Lattice parameters, atomic position, isotropic thermal vibration coefficients, preferred orientation parameters (spherical harmonics approach) are refined. Details concerning these measurements and Rietveld refinement were reported in the past for the single temperature of 300 °C (Supporting materials: ref. [21]).

## 3. Results and Discussion

Fig. 2 depicts the weight percentage of magnetite evaluated by XRD Rietveld analysis as a function of the time of hydrogen treatment at 300 °C, 340 °C and 360 °C. At constant pressure of 11 bars, temperature increase reduces the required reaction time significantly to reach a desired magnetite conversion value. While at 300 °C, 30 h are necessary to achieve a conversion above 80%, only 10 h are needed to convert the entire hematite particles batch to magnetite ones at 360 °C. We fitted the three obtained conversion curves using the Avrami model that describes the kinetics of phase transformation of a solid under isothermal conditions (Fig. 3). The values of the parameters  $n$  and  $k$  of the Avrami model are given in Table 1. While the parameter  $n$  of this model is difficult to interpret and is often seen as a fitting parameter without precise mechanistic meaning,  $k$  is usually interpreted as a rate constant describing, in the present case, the kinetics of phase transformation of the hematite into magnetite. By fitting the Arrhenius equation, thereby expressing the natural logarithm of the rate constant as a function of  $1/T$  presented in Fig. 4, the slope  $-E_a/R$  and  $E_a$  (activation energy) can be extracted,  $T$  being the temperature in Kelvin and  $R$  the gas constant.  $E_a$  is estimated to 110.77 kJ/mol.

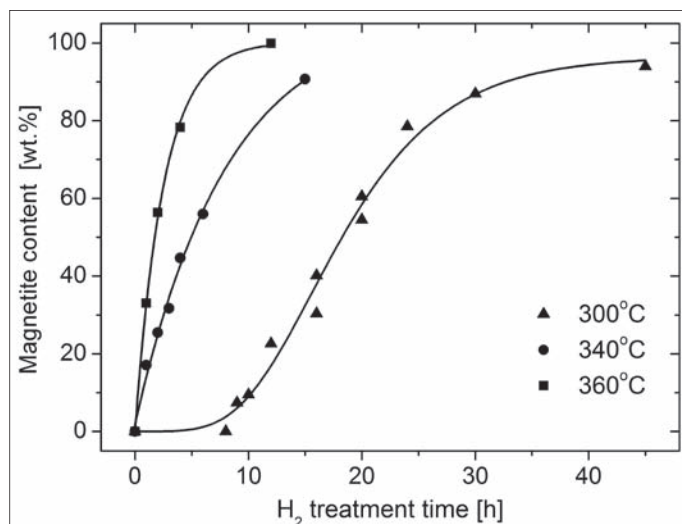


Fig. 2. Magnetite content as a function of the treatment time at different temperatures.

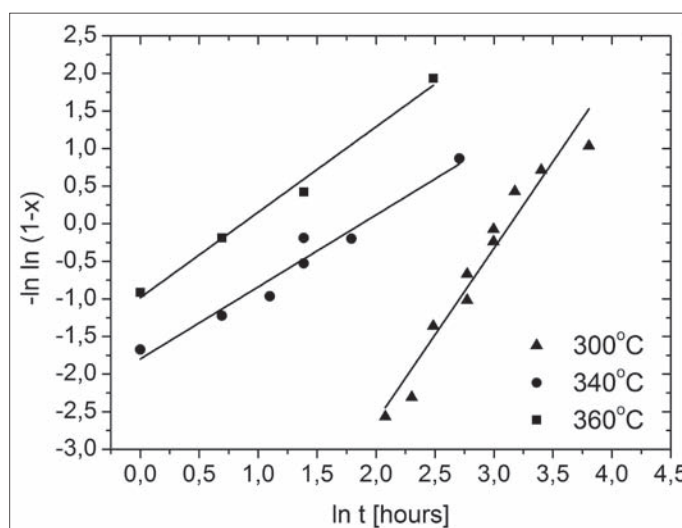


Fig. 3. Linearization of the Avrami model.  $X$  is the magnetite content expressed as a weight fraction, and  $n$  and  $k$  are the model parameters evaluated through linear fit over experimental data.  $k$  represents the rate constant of the phase transformation from hematite to magnetite.

The influence of the hydrogen reduction treatment on the Table 1. Kinetics parameters for Avrami equation modeling phase transition of a solid under isothermal conditions. The parameter  $n$  is dimensional and rate constant  $k$  is expressed in consistent SI units.

Temperature [K]	$n$ [-]	$k$ [SI units]
473	2.30	$4.32 \times 10^{-2}$
513	0.96	$15.29 \times 10^{-2}$
533	1.14	$42.10 \times 10^{-2}$

morphology evolution of the nanoparticles using 11 bars, at the three different temperatures, is depicted in Fig. 5. Micrographs show a destructive influence of temperature on particle morphology as the temperature is increased. Fig. 5 compares the spindle-type morphology from the original obtained hematite nanoparticles (Fig. 5A) before the hydrogen reduction treatment with the treatment to reach a high conversion into magnetite at 300 °C (Fig. 5B), 340 °C (Fig. 5C) and 360 °C (Fig. 5D). Fig. 5B reveals that a collapse of the porous morphology of the original

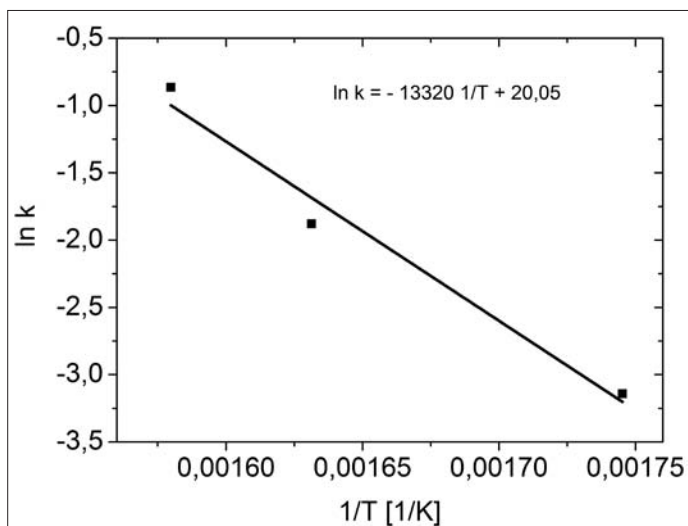


Fig. 4. Logarithm of the rate constant  $k$  as a function of  $1/T$ , where  $T$  is the temperature (in K). This graphic is a linearization of the Arrhenius equation. Activation energy ( $E_a$ ) of the phase transformation is obtained through the slope of the linear behavior.

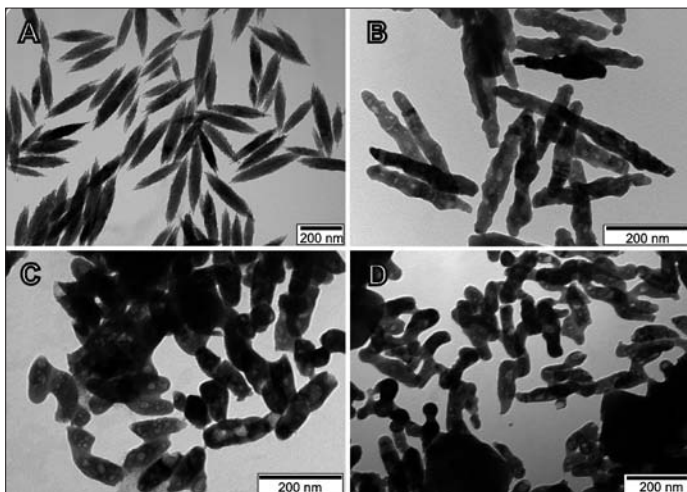


Fig. 5. TEM images depicting the morphology evolution of the hematite/magnetite hybrid nanoparticles (A) Initial hematite spindles, (B) after 30 h at 11 bar and 300 °C (87 wt%  $\text{Fe}_3\text{O}_4$ ), (C) after 15 h at 11 bar and 340 °C (91 wt%  $\text{Fe}_3\text{O}_4$ ), (D) after 15 h at 11 bar and 360 °C (100 wt%  $\text{Fe}_3\text{O}_4$ ).

hematite occurred at 300 °C. Qualitatively, the morphology is preserved with a shrinkage of the dimensions corresponding to about 15%.<sup>[21]</sup> At this stage, it seems that the surface of the nanoparticles becomes more porous and deformation of the original shape is consequently observed. XRD analysis combined with Rietveld refinement are used to evaluate the conversion of hematite to magnetite which is estimated to 87% after 30 h of treatment with hydrogen in this first example. Figs 5C and 5D show the most dramatic changes in morphology of the spindles for the highest temperatures of 340 °C and 360 °C. At these temperatures, the structure of the nanoparticles, transformed with over 90% conversion, collapses and the morphology of initial hematite nanoparticles is permanently lost. Under these conditions, there is a strong decrease in the aspect ratio of the nanoparticles associated with the transformation to magnetite. While XRD analysis estimates an almost complete conversion at 360 °C after 12 h of treatment, morphology changes are dramatic. Temperature is not the single parameter, the high pressure of 11 bars strongly influences these morphology changes. It has been shown in past experiments that after a treatment of 10–120 min at 360 °C in an oven at atmospheric pressure with a continuous flow

of hydrogen, no clear change in particle morphology is observed.<sup>[19]</sup> Therefore, the influence of pressure in the deformation mechanism of the hematite spindles is likely to be significant and experiments with different pressure levels are in progress.

#### 4. Conclusions

Kinetic studies confirm the influence of the temperature on the rate of transformation of the hematite core of spindle-shaped nanoparticles to magnetite. Increasing temperature for the reduction process from 300 °C to 360 °C allows the time of the process to be decreased to reach an equivalent (almost full) conversion of hematite phases into magnetite ones by a factor three. A negative influence of this higher temperature on the maintenance of the particle morphology is observed. If morphology seems to be affected by the crystalline transformation of hematite to magnetite, the preliminary experiments of Malik<sup>[19]</sup> suggest that the pressure influences the process in a non-negligible way and, therefore, is a matter of concern. The porous structure of the hematite is probably the reason for the observed deformations due to temperature and/or pressure.

To conclude, the adjustment of the magnetic properties of hematite nanoparticles is in principle possible and demonstrated in previous publications.<sup>[19,22]</sup> However, the conditions to operate the process, at scales opening up application-level perspectives oriented towards industry, demand further study to optimize the hydrogen pressure parameter.

#### Acknowledgements

This work is supported by the Sciex-NMS<sup>ch</sup> (Project Code 10.007), and the Adolphe Merkle Foundation.

Received: October 23, 2011

- [1] M. Ocaña, M. P. Morales, C. J. Serna, *J. Colloid Interface Sci.* **1999**, *212*, 317.
- [2] L.-H. Han, H. Liu, Y. Wei, *Powder Technol.* **2011**, *207*, 42.
- [3] W.-W. Wang, J.-L. Yao, *Mater. Res. Bull.* **2010**, *45*, 1672.
- [4] H. Dietsch, V. Malik, M. Reufer, C. Dagallier, A. Shalkevich, M. Saric, T. Gibaud, F. Cardinaux, F. Scheffold, A. Stradner, P. Schurtenberger, *Chimia* **2008**, *62*, 805
- [5] R. M. Cornell, 'The Iron Oxides: Structures, Properties, Reactions, Occurrences and Uses', Wiley-VCH, Weinheim, **2003**.
- [6] C. Rufier, M. Reufer, H. Dietsch, P. Schurtenberger, *Langmuir* **2011**, *27*, 6622.
- [7] M. Reufer, H. Dietsch, U. Gasser, B. Grobety, A. M. Hirt, V. K. Malik, P. Schurtenberger *J. Phys. Cond. Matter*, **2011**, *23*, 065102.
- [8] M. Z. Kassaee, H. Masroufi, F. Movahedi, *Appl. Catal. A* **2011**, *395*, 28.
- [9] J. Penuelas, A. Ouerghi, C. Andreazza-Vignolle, J. Gierak, E. Bourhis, P. Andreazza, J. Kiermaier, T. Sauvag, *Nanotechnology* **2009**, *20*, 425304.
- [10] C. S. S. R. Kumar, F. Mohammad, *Adv. Drug Deliv. Rev.* **2011**, *63*, 789.
- [11] G. P. Hatch, R. E. Stelter, *J. Magn. Magn. Mater.* **2001**, *225*, 262.
- [12] D. Roy, J. N. Cambre, B. S. Sumerlin, *Prog. Polym. Sci.* **2010**, *35*, 278.
- [13] C. Dagallier, H. Dietsch, P. Schurtenberger, F. Scheffold, *Soft Matter* **2010**, *6*, 2174.
- [14] A. Sanchez-Ferrer, M. Reufer, R. Mezzenga, P. Schurtenberger, H. Dietsch, *Nanotechnology* **2010**, *21*, 185603.
- [15] A. Sanchez-Ferrer, R. Mezzenga, H. Dietsch, *Macromol. Chem. Phys.* **2011**, *212*, 627.
- [16] P. Guo, Z. Wei, B. Wang, Y. Ding, H. Li, G. Zhang, X. S. Zhao, *Colloid Surface. A* **2011**, *380*, 234.
- [17] H. Itoh, T. Sugimoto, *J. Colloid Interf. Sci.* **2003**, *265*, 283.
- [18] L. Rossi, S. Sacanna, W. T. M. Irvine, P. M. Chaikin, D. J. Pine, A. P. Philipse, *Soft Matter* **2011**, *7*, 4139.
- [19] V. Malik, PhD thesis University of Fribourg, **2010**.
- [20] M. Reufer, H. Dietsch, U. Gasser, A. Hirt, A. Menzel, P. Schurtenberger, *J. Phys. Chem. B* **2010**, *114*, 4763.
- [21] I. Bobowska, S. Hengsberger, A. Hirt, B. Grobety, E. Vanoli, T. Chappuis, H. Dietsch, *Langmuir* **2011**, submitted.
- [22] A. Pineau, N. Kanari, I. Gaballah, *Thermochimica Acta* **2006**, *447*, 89.